# UNIVERSITY OF BIRMINGHAM

## Research at Birmingham

# Insight into the composition of organic compounds (> C6) in PM2.5 in Wintertime in Beijing

Lyu, Ruihe; Shi, Zongbo; Alam, Mohammed Salim; Wu, Xuefang; Liu, Di; Vu, Van Tuan; Stark, Christopher; Fu, Pingqing; Feng, Yinchang; Harrison, Roy

Link to publication on Research at Birmingham portal

Atmospheric
Chemistry
and Physics

# Insight into the composition of organic compounds ($\geq$ C$_6$) in PM$_{2.5}$ in wintertime in Beijing, China

**Ruihe Lyu[1,2,a], Zongbo Shi[2], Mohammed Salim Alam[2], Xuefang Wu[2,4], Di Liu[2], Tuan V. Vu[2], Christopher Stark[2], Pingqing Fu[3], Yinchang Feng[1], and Roy M. Harrison[2,5]**

[1]State Environmental Protection Key Laboratory of Urban Ambient Air Particulate Matter Pollution Prevention and Control, College of Environmental Science and Engineering, Nankai University, Tianjin 300350, China
[2]Division of Environmental Health and Risk Management, School of Geography, Earth and Environmental Sciences, University of Birmingham, Edgbaston, Birmingham B15 2TT, UK
[3]Institute of Surface Earth System Science, Tianjin University, Tianjin 300350, China
[4]Regional Department of Geology and Mineral Resources, China University of Geosciences, Xueyuan Road 29, 100083 Beijing China
[5]Centre of Excellence in Environmental Studies/Department of Environmental Sciences, King Abdulaziz University, P.O. Box 80203, Jeddah, 21589, Saudi Arabia
[a]now at: College of Resource and Environmental Sciences, Hebei Normal University for Nationalities, Chengde 067000, China

**Correspondence:** Roy M. Harrison (r.m.harrison@bham.ac.uk)

**Abstract.** Organic matter is a major component of PM$_{2.5}$ in megacities. In order to understand the detailed characteristics of organic compounds ($\geq$ C$_6$) at a molecular level on non-haze and haze days, we determined more than 300 organic compounds in the PM$_{2.5}$ from an urban area of Beijing collected in November–December 2016 using two-dimensional gas chromatography coupled to time-of-flight mass spectrometry (GC × GC-ToF-MS). The identified organic compounds have been classified into groups, and quantitative methods were used to calculate their concentrations. Primary emission sources make significant contributions to the atmospheric organic compounds, and six groups (including n-alkanes, polycyclic aromatic hydrocarbons – PAHs, levoglucosan, branched alkanes, n-alkenes and alkyl-benzenes) account for 66 % of total identified organic compound mass. In addition, PAHs and oxygenated PAHs (O-PAHs) were abundant amongst the atmospheric organic compounds on both haze and non-haze days. The most abundant hydrocarbon groups were observed with a carbon atom range of C$_{19}$–C$_{28}$. In addition, the total concentration of unidentified compounds present in the chromatogram was estimated in the present study. The total identified compounds account for ap-

proximately 47 % of total organic compounds ($\geq$ C$_6$) in the chromatogram on both the non-haze and haze days. The total mass concentrations of organic compounds ($\geq$ C$_6$) in the chromatogram were 4.0 and 7.4 µg m$^{-3}$ on the non-haze and haze days, respectively, accounting for 26.4 % and 18.5 % of organic matter, respectively, on those days estimated from the total organic carbon concentration. Ratios of individual compound concentrations between haze and non-haze days do not give a clear indication of the degree of oxidation, but the overall distribution of organic compounds in the chromatogram provides strong evidence that the organic aerosol is less GC volatile and hence more highly oxidized on haze days.

## 1 Introduction

China is suffering from severe PM$_{2.5}$ pollution, especially in its capital, with the annual average concentration of PM$_{2.5}$ in Beijing being in the range 69.7–122 µg m$^{-3}$ from 2000 to 2015 (Lang et al., 2017), 2.0–3.5 times the national standard (35 µg m$^{-3}$). A recent study showed that the average PM$_{2.5}$

concentration during the haze days was $256\,\mu\text{g m}^{-3}$ in the winter period from 1 to 31 December 2015 in Beijing, much higher than that on non-haze days ($24.7\,\mu\text{g m}^{-3}$; Li et al., 2019) and 25 times the World Health Organization (WHO) guideline of $10\,\mu\text{g m}^{-3}$.

Organic matter is a large and important fraction of atmospheric fine particles, and a substantial number of organic compounds can be found in the atmospheric particulate phase and may originate as either primary emissions or from the secondary formation process (Wu et al., 2018). The primary emission tracers and precursor compounds have been extensively studied in the Beijing aerosol and showed significant contributions from coal combustion, biomass burning and traffic emissions (Ren et al., 2016; Yao et al., 2016). These studies concentrated on the identification of individual organic compounds from the organic aerosol, such as n-alkanes, n-alkenes, polycyclic aromatic hydrocarbons (PAHs) and hopanes, but the structurally specific identification of the chemical composition of the organic aerosol is far from complete. Due to its huge complexity, particulate organic matter is still inadequately characterized up to the present. Hence, the identification of organic compounds in generic groups may be more informative in elucidating the molecular distribution of atmospheric organic compounds and bulk aerosol characteristics (Alam et al., 2018). Previous studies have shown that the organic compounds were highly oxidized during haze days, and secondary formation has made a significant contribution to the particulate matter (PM) (Li et al., 2019). However, these studies focused only on specific individual oxidized organic compounds or the ratios of C, N and O to assess the entire aerosol ageing process (Li et al., 2019), and the relationship between the molecular distribution and oxidizing processes during haze formation is still not clear.

Two-dimensional gas chromatography (GC × GC) coupled with time-of-flight mass spectrometry (ToF-MS) offers much enhanced resolution of complex mixtures, and the technique has been extended in the last 10 years to encompass atmospheric analysis. The two independent analytical dimensions in GC × GC-ToF-MS make this technique potentially ideal for measuring the organic components within a complex matrix such as ambient particulate matter (Hamilton et al., 2004; Welthagen et al., 2003), and its ability to separate complex mixtures of organics at low concentrations makes it an ideal technique to measure partially oxidized, isomeric and homologous series compounds, and even groups of compounds (Alam et al., 2016a; Alam and Harrison, 2016; Hamilton et al., 2004). In an earlier study of organic compounds in the Beijing atmosphere, Zhou et al. (2009) reported that 68.4 % of particulate organic matter was in the previously "unresolved complex mixture" found in conventional GC separations. The GC × GC technique is able to resolve and identify the components contributing to the unresolved mixture, and the molecular distribution of atmospheric organic compounds can be clearly identified in the chromatogram.

In order to establish relationships between organic compounds in fine particles and their characteristics on non-haze and haze days, as well as to identify the relative importance of their emission sources, further investigation of particulate organic matter composition was conducted. The objective of this study was to investigate the organic compounds with a carbon number higher than C$_6$ in PM$_{2.5}$ samples collected in central Beijing during wintertime 2016. In this paper, particle samples were analysed by the GC × GC-ToF-MS technique after solvent extraction, and the detailed organic composition was observed for polar and non-polar organic compound groups. Here, we report a large number of organic compounds and their concentrations and molecular distributions sampled on non-haze and haze days. The characteristics of the molecular distribution of atmospheric organic compounds on non-haze days were analysed and compared with haze days during aerosol ageing. In addition, we report their possible sources and formation processes and reveal and assess their pollution characteristics during non-haze and haze periods. Finally, the mass of unidentified organic compounds ($> \text{C}_6$) is estimated and compared between non-haze and haze days.

## 2 Materials and methods

### 2.1 Sampling method and site characteristics

This work was part of the APHH-Beijing study; an overview is provided by Shi et al. (2019). PM$_{2.5}$ samples were collected at the Institute of Atmospheric Physics (IAP), Chinese Academy of Sciences, in Beijing, China. The sampling site (39°58′ N, 116°22′ E) was located between North 3rd Ring Road and North 4th Ring Road. The site is approximately 1 km from 3rd Ring Road, 200 m west of the G6 Expressway (which runs north–south) and 50 m south of Beitucheng West Road (which runs east–west). The annual average vehicular speeds in the morning and evening traffic peak were 27.4 and $24.3\,\text{km h}^{-1}$, respectively. No industrial sources were located in the vicinity of the sampling site. The experimental campaign took place from 9 November to 11 December 2016. The samples were collected onto pre-baked quartz fibre filters (Pallflex) by a gravimetric high-volume sampler (Tisch, USA) with a PM$_{2.5}$ inlet at a flow rate of $1.0\,\text{m}^3\,\text{min}^{-1}$ during the sampling period. The collecting time was 24 h per sample, and three blank samples were collected during this period. The filters were previously enveloped with aluminium foils and then baked at 450 °C for 6 h before sampling. After sampling, each filter was packed separately and stored in a refrigerator below −20 °C until the analysis.

## 2.2 Analytical instrumentation

The sample extracts were analysed using a 2-D gas chromatograph (GC, 7890A, Agilent Technologies, Wilmington, DE, USA) equipped with a Zoex ZX2 cryogenic modulator (Houston, TX, USA). The first dimension was separated on a SGE DBX5, non-polar capillary column (30.0 m; 0.25 mm inner diameter; 0.25 mm – 5.00 % phenyl polysilphenylene-siloxane), and the second-dimension column was an SGE DBX50 (4.0 m; 0.10 mm inner diameter; 0.10 mm – 50.0 % phenyl polysilphenylene-siloxane). The GC × GC was interfaced with a BenchTOF-Select time-of-flight mass spectrometer (Markes International, Llantrisant, UK). The acquisition speed was 50.0 Hz, with a mass resolution of > 1200 FWHM (full width at half maximum) at 70.0 eV, and the mass range was $m/z$ 35.0 to $m/z$ 600. All data produced were processed using GC Image version 2.5 (Zoex Corporation, Houston, TX, USA).

## 2.3 Extraction and analysis methods of filters

The filters were spiked with 30.0 μL of 30.0 μg mL$^{-1}$ deuterated internal standards (pentadecane-d$_{32}$, eicosane-d$_{42}$, pentacosane-d$_{52}$, triacontane-d$_{62}$, butylbenzene-d$_{14}$, nonylbenzene-2,3,4,5,6-d$_5$, biphenyl-d$_{10}$ and p-terphenyl-d$_{14}$; Sigma-Aldrich, UK) for quantification and then immersed in methanol/dichloromethane (DCM) (1 : 1, $v/v$) and ultra-sonicated for 20 min at 20 °C. The extract was filtered using a clean glass pipette column packed with glass wool and anhydrous Na$_2$SO$_4$ and concentrated to 100 μL under a gentle flow of nitrogen for analysis using GC × GC-ToF-MS; 1 μL of the extracted sample was injected in a split ratio of 50 : 1 at 300 °C. The initial temperature of the primary oven (80 °C) was held for 2 min and then increased at 2 °C min$^{-1}$ to 210 °C, followed by 1.5 °C min$^{-1}$ to 325 °C. The initial temperature of the secondary oven (120 °C) was held for 2 min and then increased at 3 °C min$^{-1}$ to 200 °C, followed by 2 °C min$^{-1}$ to 300 °C and a final increase of 1 °C min$^{-1}$ to 330 °C to ensure that all species passed through the column. The transfer line temperature was 330 °C, and the ion source temperature was 280 °C. Helium (99.999 %) was used as the carrier gas at a constant flow rate of 1 mL min$^{-1}$. Further details of the instrumentation and data-processing methods are given by Alam and Harrison (2016) and Alam et al. (2016a).

## 2.4 Qualitative and quantitative analysis

Standards used in these experiments included 26 n-alkanes (C$_{11}$ to C$_{36}$), EPA's 16 priority-pollutant PAHs, 4 hopanes (17$\alpha$(H),21$\beta$(H)-22R-homohopane, 17$\alpha$(H),21$\beta$(H)-hopane, 17$\alpha$(H),21$\beta$(H)-30-norhopane and 17$\alpha$(H)-22,29,30-trisnorhopane), 7 decalins and tetralines (cis- and trans-decalin, tetralin, 5-methyltetraline, 2,2,5,7-tetramethyltetraline, 2,5,8-trimethyltetraline, and 1,4-dimethyltetraline), 4 alkyl-naphthalenes (1-methyl-naphthalene, 1-ethyl-naphthalene, 1-n-propyl-naphthalene and 1-n-hexyl-naphthalene), 13 alkyl-cyclohexanes (n-heptyl-cyclohexane to n-nonadecyl-cyclohexane), 5 alkyl-benzenes (n-butyl-benzene, n-hexyl-benzene, n-octyl-benzene, n-decyl-benzene and n-dodecyl-benzene; Sigma-Aldrich, UK; purity > 99.2 %), 11 n-aldehydes (C$_8$ to C$_{13}$; Sigma-Aldrich, UK; purity $\geq$ 95.0 %), C$_{14}$ to C$_{18}$ (Tokyo Chemical Industry UK Ltd; purity > 95.0 %), 11 2-ketones, C$_8$ to C$_{13}$ and C$_{15}$ to C$_{18}$ (Sigma-Aldrich, UK; purity $\geq$ 98.0 %), C$_{14}$ (Tokyo Chemical Industry UK Ltd; purity 97.0 %), 4 n-alcohols (2-decanol, 2-dodecanol, 2-hexadecanol and 2-nonadecanol; Sigma-Aldrich, UK; purity 99.0 %), and 1-pentadecanol (Sigma-Aldrich, UK; purity 99.0 %).

Compound identification was based on the GC × GC-ToF-MS spectral library, NIST mass spectral library and co-injection with authentic standards. Compounds within the homologous series for which standards were not available were identified by comparing the retention time interval between homologues, by comparison of mass spectra with the standards for similar compounds within the series, by comparison to the NIST mass spectral library and by the analysis of fragmentation patterns. The quantification for identified compounds was performed by the linear regression method using the seven-point calibration curves (0.05, 0.10, 0.25, 0.50, 1.00, 2.00 and 3.00 ng μL$^{-1}$) established between the concentration ratios of authentic standards to internal standards and the corresponding peak area ratios. The calibration curves for all target compounds were highly linear ($r^2$ > 0.98; from 0.978 to 0.998), demonstrating the consistency and reproducibility of this method. Limits of detection for individual compounds were typically in the range 0.001–0.08 ng m$^{-3}$. The identified compounds which have no commercial authentic standards were quantified using the calibration curves for similar structure compounds or isomeric compounds. This applicability of quantification of individual compounds using isomers of the same compound functionality (which have authentic standards) has been discussed elsewhere and has a reported uncertainty of 24 % (Alam et al., 2018).

The branched alkanes, alkyl-benzenes, alkyl-decalins, alkyl-phenanthrene and anthracene (alkyl-Phe and Ant), alkyl-naphthalene (alkyl-Nap), and alkyl-benzaldehyde were identified in the samples with the graphics method of the GC Image version 2.5 (Zoex Corporation, Houston, TX, USA), and the detailed descriptions are given elsewhere (Alam et al., 2018). Briefly, the structurally similar compounds (similar physico-chemical properties) were identified as a group via drawing a polygon around a section of the chromatogram with the polygon selection tool. All compounds included in the polygon belong to a special compound class, and the total concentrations were calculated via a calibration curve of the adjacent compounds and internal standards (ISs).

Field and laboratory blanks were routinely analysed to evaluate analytical bias and precision. Blank levels of indi-

vidual analytes were normally very low and, in most cases, not detectable. The major contaminants observed were very minor amounts of n-alkanes ranging from $C_{11}$ to $C_{21}$, with no carbon number predominance and maximum at $C_{18}$; PAH was not detectable. The major proportion of the contaminants could be distinguished by its low concentrations and distribution fingerprints (especially the n-alkanes). These contaminants did not interfere with the recognition or quantification of the compounds of interest. Recovery efficiencies were determined by analysing the blank samples spiked with standard compounds. Mean recoveries ranged between 82 % and 98 %. All quantities reported here have been corrected according to their recovery efficiencies. Analytical data from the GC × GC analysis were compared with a conventional GC–MS analysis for levoglucosan and 13 PAH. The results from two analytical instruments were compared, and the correlations ($r^2$) between them were in the range of 0.5 to 0.8, with 10 mean concentrations of individual compounds from each technique within 20 % of one another, 2 within 20 %–30 %, and the remainder (2) within 30 %–40 % of one another. The largest outlier was levoglucosan, which was underestimated, probably since it decomposed due to a lack of the usual derivatization.

## 3   Results and discussion

### 3.1   General aerosol characteristics

Thirty-three samples were separated into non-haze (13) and haze (20) days (the latter with PM$_{2.5}$ exceeding 75 μg m$^{-3}$ for 24 h average) according to the National Ambient Air Quality Standards of China (NAAQS) report released in 2012 by the Ministry of Environmental Protection (MEP) of the People's Republic of China. The concentrations of PM$_{2.5}$, black carbon (BC), organic carbon (OC), element carbon (EC), gaseous pollutants (SO$_2$, NO, NO$_2$, NO$_x$ and CO) and meteorological parameters (wind speed – WS, wind direction – WD – and relative humidity – RH) were simultaneously determined during the field campaigns and appear in Table S1 in the Supplement.

The average daily PM$_{2.5}$ mass was 99 μg m$^{-3}$, and that on haze days (average 141 μg m$^{-3}$) was 4 times higher than that on non-haze days (35.3 μg m$^{-3}$). The wind and temperature during the haze and non-haze days were 0.94 and 1.44 m s$^{-1}$ and 6.1 and 4.0 °C, respectively. However, the relative humidity during haze episodes (56.3 %) was slightly higher than the non-haze periods (39.8 %). The concentrations of gaseous pollutants SO$_x$, NO$_x$ and CO were simultaneously elevated with the increase in PM$_{2.5}$ concentrations, whereas the O$_3$ concentration presented an opposite trend to PM$_{2.5}$ concentrations (Shi et al., 2019). The average concentration of organic matter (OM) was estimated as 30.2 μg m$^{-3}$ using the OC concentration (18.9 μg m$^{-3}$) and a multiplying factor of 1.6 for aged aerosols (Turpin and Lim, 2001). The OM

concentration was 40.0 and 15.0 μg m$^{-3}$ on haze and non-haze days, respectively.

### 3.2   The major classes of organic compounds in PM$_{2.5}$

More than 6000 peaks were found in the 2-D chromatogram image of each sample by the data-processing software (GC Image version 2.5). Over 300 polar and non-polar organic compounds (POCs and N-POCs) were identified and quantified in the PM$_{2.5}$ samples, and these compounds are grouped into more than 20 classes, including normal and branched alkanes, n-alkenes, aliphatic carbonyl compounds (1-alkanals, n-alkan-2-ones and n-alkan-3-ones), n-alkanoic acids, n-alkanols, PAHs, oxygenated PAHs (O-PAHs), alkylated-PAHs, hopanes, alkylbenzenes, alkyl-cyclohexanes, pyridines, quinolines, furanones, and biomarkers (levoglucosan, cedrol, phytane, pristane, supraene and phytone). The details of aliphatic hydrocarbon measurements (including n-alkanes and n-alkenes) and carbonyl compounds (including n-alkanals, n-alkan-2-ones, n-alkan-3-ones, furanones and phytone) were reported in previous papers (Lyu et al., 2019a, b). The total concentrations of identified organic compounds ranged from 0.94 to 5.14 μg m$^{-3}$, with the average of 2.84 ± 1.19 μg m$^{-3}$, accounting for 9.40 % of OM. The concentrations of identified individual organic compounds are summarized in Table S2, and the percentage of each group in the total identified organic compounds is in Fig. 1. The n-alkanes (16 %) make the greatest contribution to the total mass of identified organic compounds, followed by levoglucosan (13 %), branched alkanes (13 %), PAHs (10 %), n-alkenes (7 %) and alkylbenzenes (7 %). These six groups account for 66 % of total identified organic compounds by mass and a total concentration of 1.41 μg m$^{-3}$, accounting for 1.42 % of the particle mass. In a study in Nanjing, Haque et al. (2019) reported the most abundant classes of organic compounds to be n-alkanes (205 ng m$^{-3}$), followed by fatty acids (76.3 ng m$^{-3}$), PAHs (64.3 ng m$^{-3}$), anhydrosugars (levoglucosan, galactosan and mannosan; 56.3 ng m$^{-3}$), fatty alcohols (40.5 ng m$^{-3}$) and phthalate esters (15.2 ng m$^{-3}$).

### 3.3   The characteristics of organic compound groups on non-haze and haze days

The average total concentration of identified groups was calculated for the non-haze (13 d) and haze periods (20 d). The comparisons of two periods (non-haze and haze days) are shown in Fig. 2, and the detailed concentrations of each group are shown in the Table S3. The concentrations of most organic compound groups on the haze days were higher than non-haze days, especially for the n-alkanols and n-$C_n$-cyclohexanes. The alkyl-benzenes, alkyl-benzaldehydes, monoaromatic compounds and quinoline have approximately similar concentrations on the non-haze and haze days.
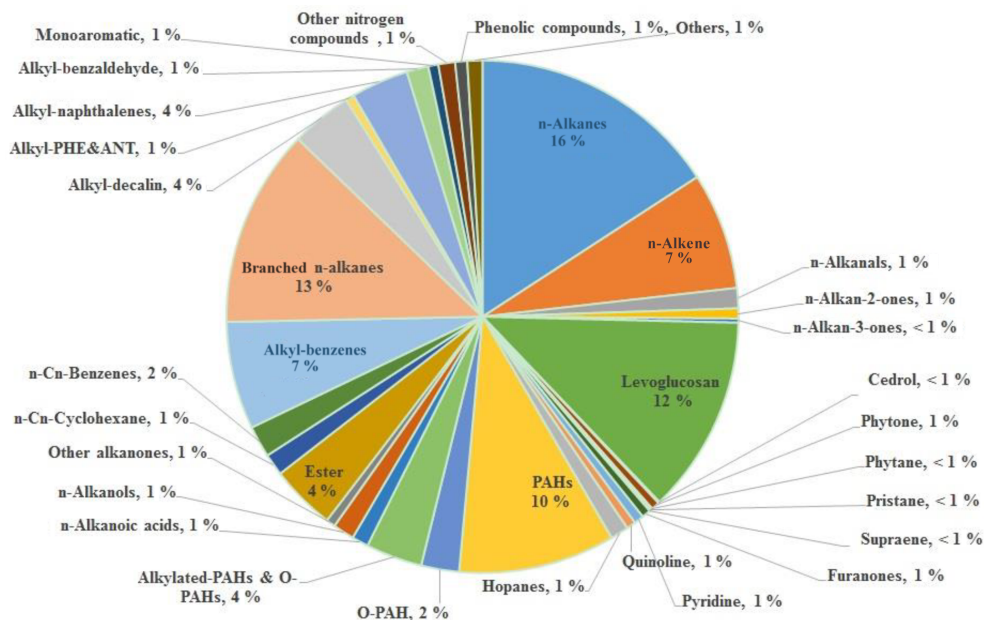
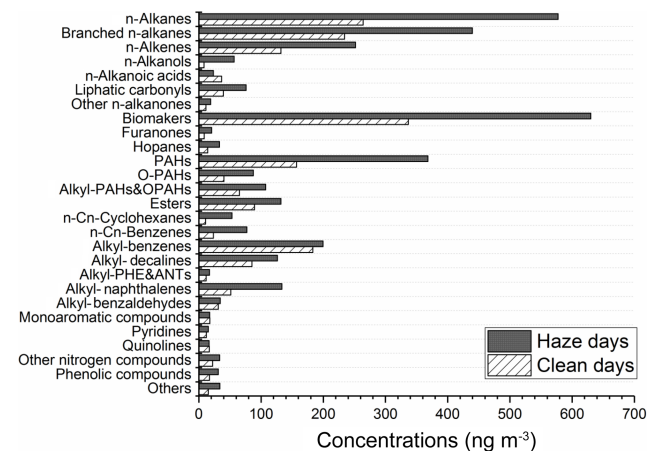**Figure 1.** The percentages of the organic compound groups in the total identified organic compounds.



**Figure 2.** A comparison of organic compound groups between non-haze and haze days. The average total concentration of the identified group was calculated in the non-haze (13 d) and haze periods (20 d).

As many compound groups have not been reported in previous studies, and complete data on the relative abundance of these compounds in various source emissions are not available at present, it is not yet possible to calculate source contributions to ambient organic compound concentrations via molecular marker or mathematical modelling methods. However, several important consistency checks on the potential source can be performed. In the sections that follow, the literature on the origin of each of these compound classes is reviewed briefly and the measured compound concentrations are described. Table 1 shows the comparison of identified organic compounds between the present and previous studies in

Beijing. In many but not all cases, concentrations are comparable.

### 3.3.1 n-Alkanoic acids, n-alkanols and carbonyl compounds

The n-alkanoic acids with carbon numbers from C$_6$ to C$_{10}$ were identified in the PM$_{2.5}$. Higher-molecular-weight (HMW) alkanoic acids generated from the biomass burning (Simoneit and Mazurek, 1982) were not identified from the samples, probably due to low volatility in the GC. The n-alkanoic acids were observed at a similar magnitude to a previous study in Beijing (Zhou et al., 2009; Table 1).

Previous studies have found that the n-alkanoic acid homologues were significantly impacted by cooking emissions in Beijing and showed higher concentrations on non-haze days and a similar distribution pattern in all seasons (Huang et al., 2006; He et al., 2006; Sun et al., 2013). Consistent results for acids were observed in this study, and the $\sum$ n-alkanoic acids had an average concentration on the non-haze days of 36.4 ng m$^{-3}$, higher than 24.6 ng m$^{-3}$ on haze days, strongly implying a dominant contribution from cooking emissions as opposed to secondary formation.

In the present study, 1-alkanols with even-carbon numbers from C$_{12}$ to C$_{20}$ were identified in the PM$_{2.5}$, with a quite similar molecular distribution to that of diesel engine exhaust samples (Alam et al., 2016b). In addition, other primary emission sources may make a potential contribution to these compounds, including those from biomass burning (Zhang et al., 2007). The average $\sum$ n-alkanol concentration was 38.5 ng m$^{-3}$, and $\sum$ n-alkanols had higher concentrations on the haze days (59.8 ng m$^{-3}$), approximately 8 times

**Table 1.** Comparison of identified organic compounds with earlier studies in Beijing. Data from the present study are mean $\pm$ standard deviation for $n = 33$ samples.

| Compound name | Concentrations (ng m$^{-3}$) | |
| --- | --- | --- |
| | Present | Previous study |
| **n-Alkanols** | | |
| 1-Dodecanol | $2.27 \pm 1.49$ | 0.90[j]; |
| 1-Tetradecanol | $24.2 \pm 88.9$ | 3.00[j]; |
| 1-Hexadecanol | $6.66 \pm 20.7$ | 1.2[d]; 6.30[j]; |
| 1-Octadecanol | $1.69 \pm 1.65$ | 3.1[d]; 20.1[j]; |
| 1-Eicosanol | $3.71 \pm 2.96$ | 19.5[j]; |
| **n-Alkanoic acids** | | |
| Hexanoic acid | $1.80 \pm 1.54$ | 30.4[i]; 0.00[j]; |
| Heptanoic acid | $0.73 \pm 1.05$ | 0.62[j]; |
| Octanoic acid | $2.97 \pm 2.56$ | 29.6[i]; 0.62[j]; |
| Nonanoic acid | $1.23 \pm 1.37$ | 2.07[j]; |
| Decanoic acid | $22.8 \pm 25.2$ | 6.4[d]; 5.8[i]; 1.24[j]; |
| **Hopanes** | | |
| 18$\alpha$(H)22,29,30-Trisnorneohopane | $2.91 \pm 3.06$ | 0.22[j]; |
| 17$\alpha$(H)-22,29,30-Trisnorhopane | $1.56 \pm 2.74$ | 2.75[a]; 2.3[d]; 0.5[i]; 0.21[j]; |
| 17$\alpha$(H)21$\beta$(H)-30-Norhopane | $9.92 \pm 7.63$ | 7.19[a]; 4.1[d]; |
| 17$\beta$(H)21$\alpha$(H)-Hopane(Moretane) | $5.77 \pm 6.12$ | 1.32[j]; 1.9[d]; |
| 17$\alpha$(H)21$\beta$(H)-Hopane | $3.71 \pm 5.49$ | 3.51[a]; 3.2[d]; 0.8[i]; 1.54[j]; |
| 17$\alpha$(H)21$\beta$(H)-Homohopane(22R) | $1.32 \pm 1.31$ | 0.63[a]; 1.2[d]; 0.42[j]; |
| 17$\alpha$(H)21$\beta$(H)-Homohopane(22S) | $0.83 \pm 0.93$ | 2.94[a]; 1.2[d]; 0.63[j]; |
| 17$\alpha$(H),21$\beta$(H)-Bishomohopane(22S) | $5.23 \pm 6.51$ | 0.7[d]; |
| 17$\alpha$(H)21$\beta$(H)-Bishomohopane(22R) | $1.41 \pm 1.73$ | 0.7[d]; |
| Subtotal | $32.7 \pm 24.7$ | |
| **PAHs** | | |
| Naphthalene (NAP; two rings) | $6.03 \pm 4.52$ | 0.22[b]; 2.4[i]; |
| Acenaphthylene (ACY; two rings) | $12.7 \pm 9.93$ | 0.065[b]; 0.3[i]; |
| Acenaphthene (ACE; two rings) | $6.04 \pm 8.94$ | 0.79[b]; 0.51[g]; 0.3[i]; |
| Fluorene (FLU; three rings) | $16.6 \pm 13.0$ | 1.18[b]; 1.65[g]; 0.5[i]; 15.6[j]; |
| Phenanthrene (PHE; three rings) | $8.59 \pm 8.49$ | 14.0[b]; 0.9[d]; 1.1[e]; 21.65[f]; 30.3[g]; 0.9[i]; 95.7[j]; |
| Anthracene (ANT; three rings) | $6.14 \pm 6.53$ | 1.70[b]; 3.3[d]; 5.74[g]; 0.2[i]; 52.3[j]; |
| Pyrene (PYR; four rings) | $18.9 \pm 18.2$ | 22.3[b]; 12[d]; 0.58[e]; 31.3[f]; 64.4[g]; 1.0[i]; 235[j]; |
| Fluoranthene (FLT; four rings) | $21.0 \pm 20.4$ | 41.5[b]; 11[d]; 0.23[e]; 31.8[f]; 76.4[g]; 1.1[i]; 222[j]; |
| Chrysene (CHR; four rings) | $25.5 \pm 19.3$ | 21.8[b]; 1.00[d]; 1.00[e]; 50.6[f]; 62.7[g]; 1.3[i]; 140[j]; |
| Benz[a]anthracene (BaA; four rings) | $17.6 \pm 14.6$ | 23.5[b]; 19[d]; 43.4[f]; 45.1[g]; 0.8[i]; 62.9[j]; |
| Benzo[k]fluoranthene (BkF; four rings) | $8.81 \pm 7.68$ | 17.0[b]; 8.3[d]; 33.6[g]; 0.7[i]; 30.5[j]; |
| Cyclopenta[c,d]pyrene (CcP; five rings) | $8.60 \pm 10.2$ | 68.0[j]; |
| Perylene (PER; five rings) | $3.20 \pm 2.69$ | 2.81[b]; 14[d]; 5.99[g]; 0.2[i]; |
| Benzo[b]fluoranthene (BbF; five rings) | $38.5 \pm 31.8$ | 34.0[b]; 59[d]; 33.1[f]; 53.6[g]; 2.3[i]; 134[j]; |
| Benzo[a]pyrene (BaP; five rings) | $13.1 \pm 13.8$ | 14.6[b]; 14[d]; 0.08[e]; 40.2[f]; 28.6[g]; 1.1[i]; 41.3[j]; |
| Indeno[1,2,3-cd]pyrene (IcdP; six rings) | $12.3 \pm 8.82$ | 18.1[b]; 15.2[d]; 0.32[e]; 40.9[f]; 32.3[g]; 1.2[i]; 18.2[j]; |
| Benzo[ghi]perylene (BghiP; six rings) | $12.4 \pm 11.1$ | 12.2[b]; 12[d]; 0.33[e]; 22.2[g]; 2.6[i]; 59.0[j]; |
| Benzo[e]pyrene (BeP; five rings) | $15.4 \pm 10.3$ | 12.4[b]; 12[d]; 0.65[e]; 24.7[g]; 1.3[i]; 72.6[j]; |
| Dibenzo[a,h]pyrene (DBA; five rings) | $5.68 \pm 7.35$ | 2.01[b]; 3.1[d]; |
| Benzo[ghi]fluoranthene (BghiF; five rings) | $15.1 \pm 15.8$ | 0.08[e]; 15.3[f]; |

**Table 1.** Continued.

| Compound name | Concentrations (ng m$^{-3}$) | |
|---|---|---|
| | Present | Previous study |
| O-PAHs | | |
| Anthracenedione (AQ) | $5.12 \pm 5.97$ | $108^b$; |
| 7,12-Benz[a]anthracenequinone (BaAQ) | $4.09 \pm 3.61$ | $2.14^b$; |
| Aceanthrenequinone (AceAntQ) | $2.41 \pm 2.89$ | $0.01^b$; |
| Phenanthraquinone (PQ) | $1.45 \pm 1.08$ | $0.13^b$; |
| 9-Fluorenone (9-FluQ) | $3.78 \pm 4.01$ | $28.3^g$; |
| Alkylated-(PAHs and O-PAHs) | | |
| Pyrene, 1-methyl-(1-MePYR) | $21.5 \pm 21.5$ | $3.80^b$ |
| Phenanthrene, 1-methyl-(1-MePHE) | $5.29 \pm 5.38$ | $4.29^b$ |
| Retene | $5.39 \pm 9.72$ | $0.12^e$; $0.5^i$; |
| Ester | | |
| Dibutyl phthalate (DBP) | $16.9 \pm 15.5$ | $21^d$; $3.00^j$; |
| Diethyl phthalate (DEP) | $2.67 \pm 2.91$ | $3.5^d$; $24.0^j$; |
| Di(2-ethylhexyl)-phthalate (DEHP) | $16.0 \pm 12.6$ | $130^d$; |
| Diisobutyl phthalate | $49.7 \pm 43.2$ | $22^d$; |
| Dimethyl phthalate | $2.58 \pm 2.80$ | $1.5^d$; |
| Biomarkers | | |
| Levoglucosan | $355 \pm 232$ | $310^a$; $790.3^c$; $171^d$; $78^h$; $97.1^i$; $830^j$; |
| Phytone | $14.7 \pm 11.7$ | $0.9^j$; |
| Phytane | $1.94 \pm 1.05$ | $2.3^i$; $1.30^j$; |
| Pristane | $2.24 \pm 1.69$ | $1.8^i$; $0.67^j$; |
| Other nitrogen compounds (nitro-amine-heterocyclic compounds) | | |
| Benzo[f]quinoline | $4.40 \pm 4.66$ | $3.10^j$; |
| Isoquinoline | $0.80 \pm 0.83$ | $0.22^j$; |
| Phenolic compounds | | |
| 1-Naphthalenol (1-OH-NAP) | $1.56 \pm 5.61$ | $0.22^b$ |
| 2-Naphthalenol (2-OH-NAP) | $1.15 \pm 1.21$ | $2.74^b$ |
| 2-Dibenzofuranol (2-OHDBF) | $1.84 \pm 2.09$ | $1.47^b$ |

[a] Beijing, PKU, heating seasons (Ma et al., 2018). [b] Beijing, PKU, heating seasons (Lin et al., 2015). [c] Beijing, China University of Geosciences (Beijing), winter (Shen et al., 2018). [d] Beijing, winter of 2003 (Wang et al., 2006). [c] Beijing, urban, June (Simoneit et al., 1991). [d] Beijing, urban, haze period (Gao et al., 2016). [e] Beijing, PKU, haze period (Li et al., 2019). [f] Beijing, PKU, winter (He et al., 2006). [g] During the 2008 Beijing Olympic Games, PKU sites (Guo et al., 2013). [h] Beijing, urban, winter (Zhou et al., 2009).

greater than 8.39 ng m$^{-3}$ on non-haze days. The above results suggest that n-alkanol formation is more efficient on haze days, even though vehicular emissions appear to be another important source.

Aliphatic carbonyl compounds, including n-alkanals, n-alkan-2-ones and n-alkan-3-ones, were described in detail by Lyu et al. (2019a). Briefly, the daily sum of aliphatic carbonyls ($\sum$ AC) ranged from 8.87 to 164 ng m$^{-3}$, accounting for 0.02 %–0.46 % of OM. The average $\sum$ AC was 75.8 ng m$^{-3}$ during all haze days, approximately double the 39.5 ng m$^{-3}$ of the non-haze period. Lyu et al. (2019a)

showed that the n-alkanals were mainly originated from vehicle exhaust or formed from OH oxidation of n-alkanes, while the n-alkanones were probably emitted mainly by coal combustion.

### 3.3.2 Nitrogen-containing organic compounds

Nitrogen-containing (N-containing) organic compounds have been reported in many previous studies, and the important sources of N-containing compounds are coal combustion, biomass burning, vehicular exhaust and atmospheric photochemical reactions (Rogge et al., 1994,

1993b; Schauer et al., 1996; Zhang et al., 2002; Fan et al., 2018). N-containing compounds were identified in the samples, including heterocyclic compounds (alkyl-pyridines and alkyl-quinolines) and other N-containing compounds (nitro and amine compounds). The average $\sum$ alkyl-pyridines, $\sum$ alkyl-quinolines and $\sum$ other N-containing compounds were 17.4 ± 7.58, 16.6 ± 15.0 and 30.0 ± 23.1 ng m$^{-3}$, respectively, and the average total concentration of N-containing compounds was 64.0 ng m$^{-3}$, accounting for approximately 0.2 % of the OM.

The quinolines have been proposed for use as tracers of vehicular exhaust (Rogge et al., 1993a) and crude oils and shale oil combustions (Schmitter et al., 1983; Simoneit et al., 1971), while the straight-chain alkyl-pyridines (n-C$_n$-pyridine) are related to petrochemical industries (Botalova et al., 2009) and secondary formation from pyrolysis of proteins and amino acids under a high temperature (Chiavari and Galletti, 1992; Hendricker and Voorhees, 1998; Kögel-Knabner, 1997). This study found that both quinolines and alkyl-pyridines showed similar concentrations on the non-haze and haze days, 16.8 ± 16.5 ng m$^{-3}$ (non-haze) and 16.5 ± 14.4 ng m$^{-3}$ (haze days) and 12.0 ± 6.02 ng m$^{-3}$ (non-haze days) and 15.3 ± 8.36 ng m$^{-3}$ (haze days), respectively. Amino compounds can originate from biomass burning and coal combustion and are abundant in winter fine particulate-matter samples compared to summer (Zhang et al., 2002; Akyüz, 2008). In the present study, the average $\sum$ other N-containing compounds was 34.2 ± 24.6 ng m$^{-3}$ on the haze days, somewhat higher than 22.6 ± 19.4 ng m$^{-3}$ on non-haze days.

The similar concentrations on the non-haze and haze days suggest that N-containing organic compounds mainly originated from primary sources and are subject to degradation during the haze formation process.

Tracers of tobacco smoke, benzoquinoline and isoquinoline have previously been determined in the PM collected in Beijing, with concentrations of 3.10 and 0.22 ng m$^{-3}$, respectively (Zhou et al., 2009). These two compounds were also identified in the present study, with 4.40 and 0.80 ng m$^{-3}$, respectively. Phthalimide was identified in the PM at 0.91 ng m$^{-3}$ and was considered to be derived from cyclization and aromatization reactions of proteins or from intermediates in the transformation of carboxyl ammonium salts to nitriles by Zhao et al. (2009).

### 3.3.3 Esters

Phthalate esters are organic chemicals that are commonly used in a variety of consumer products and in various industrial and medical applications and are predominantly used as plasticizers to improve the flexibility of polyvinyl chloride (PVC) resins and other polymers. Table 1 shows a comparison of phthalate esters (DBP, DEP and DEHP) between the present and previous studies in the winter in Beijing; it seems that the concentrations of some phthalate esters have signif-
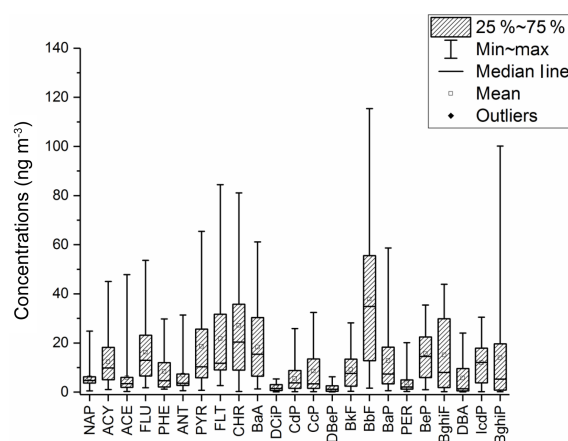


**Figure 3.** The distribution of concentrations of PAHs (shaded bars; 25 % – first quartile; 75 % – third quartile).

icantly decreased from earlier studies (Wang et al., 2006; Zhou et al., 2009). The present study found that diisodecyl phthalates, DBP and DEHP were abundant compounds in the ester group, with 49.7 ± 43.2, 16.9 ± 15.5 and 16.0 ± 12.6 ng m$^{-3}$, respectively. The DBP, DEP and DEHP in Beijing were far lower than those in winter in Tianjin (Kong et al., 2013) and another 15 cities around China (Li and Wang, 2015; Wang and Kawamura, 2005; Wang et al., 2006). In addition, the average $\sum$ ester was 117 ± 82.1 ng m$^{-3}$, with 132 ± 87.1 and 89.4 ± 70.0 ng m$^{-3}$ on haze and non-haze days, respectively. Since phthalates are not chemically bound to the polymeric matrix, they can enter the environment by escaping from manufacturing processes and by leaching or vaporizing from final products (Staples et al., 1997).

### 3.3.4 PAHs, O-PAHs and alkylated-(PAHs and O-PAHs)

In all, 23 PAHs (two–six rings), 19 oxygenated PAHs (O-PAHs) and 14 alkylated-(PAHs and O-PAHs) were determined in the PM$_{2.5}$ samples. The average total polycyclic aromatic compounds (the sum of $\sum$ PAHs, $\sum$ O-PAHs, $\sum$ alkylated-(PAHs and O-PAHs), alkyl-PHE and ANT, and alkyl-NAP) were 569 ng m$^{-3}$, accounting for 1.88 % of OM.

The distribution of PAHs is shown in Fig. 3; the most abundant PAHs were BbF, followed by CHR, FLT, BaA and PYR. In all samples, the $\sum$ PAHs ranged from 46.7 to 727 ng m$^{-3}$, with an average of 281 ± 176 ng m$^{-3}$, accounting for 0.93 % of OM. In addition, the average $\sum$ PAHs was 364 ng m$^{-3}$ during haze days but only 159 ng m$^{-3}$ on the non-haze days. It should be noted that retene was detected in most samples, with an average concentration of 14.4 ± 17.5 ng m$^{-3}$. It has been suggested that retene predominantly originates from the combustion of conifer wood (Simoneit et al., 1991).

Nineteen oxygenated PAHs (O-PAHs) make up of a class of PAH derivatives that are present in the atmosphere as a result of direct emission during combustion and secondary for-

mation by homogeneous and heterogeneous photo-oxidation processes (Keyte et al., 2013; Ringuet et al., 2012). They are also of scientific interest because they are, typically, found in the secondary organic aerosol (SOA) formed by photo-oxidation of PAH (Shakya and Griffin, 2010). In urban samples, polycyclic aromatic ketones (PAKs), polycyclic aromatic quinones (PAQs) and polycyclic aromatic furanones (PAFs) are typical groups of compounds (Lin et al., 2015). The average total concentration of O-PAH measured in this study (Fig. 4) was 67.9 ng m$^{-3}$. The polycyclic aromatic ketones 4,5-pyrenequinone (4,5-PyrQ; 8.75 ng m$^{-3}$) and 1,6-pyrenequinone (1,6-PyrQ; 7.38 ng m$^{-3}$) were the most abundant compounds during the sampling campaign. Four O-PAHs were identified previously at the Peking University (PKU) site in the 2012 heating season in Beijing (Table 1); it is notable that the concentration of AQ was up to 108 ng m$^{-3}$, approximately 20 times that in the present study (5.12 ng m$^{-3}$). As O-PAHs can be formed during sampling, it is necessary to be very careful in reconciling their presence with specific sources (Pitts et al., 1980). The average $\sum$O-PAHs was 86.5 ng m$^{-3}$ during haze days but 39.7 ng m$^{-3}$ on the non-haze days. The ratio of quinone to parent PAH has been used to assess the air mass age (Alam et al., 2014; Harrison et al., 2016). The average ratios of phenanthraquinone to phenanthrene (PQ : PHE), anthraquinone to anthracene (AQ : ANT) and benzo(a)anthracene-7,12-quinone to benzo(a)anthracene (BaAQ : BaA) were 0.37, 1.27 and 0.32, respectively, with PQ : PHE, AQ : ANT and BaAQ : BaA ratios of 0.25, 0.88 and 0.26 on the haze days, which were lower than 0.55, 1.92 and 0.40 on non-haze days. The BaAQ : BaA ratios were lower than earlier published data of 1.28 measured in Beijing (Li et al., 2019), 1.40 in Xi'an (Wang et al., 2016) and 0.54 in Beijing–Tianjin (Wang, 2010) but higher than the 0.08 measured in Guangzhou (Wei et al., 2012) and 0.09 in Zhuanghu (Ding et al., 2012). Shen et al. (2011) reported that the BaAQ : BaA ratio was 0.03 for coal combustion, 0.16 for crop residue burning (Shen et al., 2012a) and 6.6 from biomass pellet burning (Shen et al., 2012b). The low ratios of O-PAHs to PAHs in our data probably indicated that the particulate matter mainly originated from coal combustion and biomass burning. However, the lower ratios on haze days than non-haze days may imply continued oxidation of the O-PAH to products which were not analysed. Li et al. (2019) also reported that ratios of O-PAH to PAH were very similar during haze and clean-air periods, which provides support for this conclusion.

### 3.3.5 Molecular markers

The hopanes are compounds present in crude oil as a result of the decomposition of sterols and other biomass and are not by-products of combustion (Simoneit, 1985). They are very stable and have been proposed for use as tracers for atmospheric particles from fossil fuel combustion, such as motor
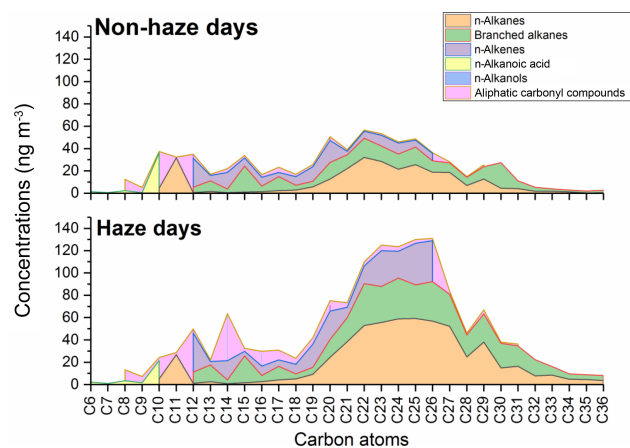


**Figure 4.** The molecular distributions of aliphatic hydrocarbons and other homologous series, including n-alkanes, branched alkanes, n-alkenes, carbonyl compounds (n-alkanals, n-alkan-2-ones and n-alkan-3-ones), n-alkanoic acid and alkanols on haze and non-haze days.

vehicle exhaust (Simoneit, 1985) and coal combustion (Oros and Simoneit, 2000). The hopanes are widely used as tracers of traffic emission due to vehicle emissions having high loadings of hopanes (Cass, 1998). The comparison of hopanes between this study and previous studies in the winter or heating season of Beijing is shown in Table 1. Hopanes were extensively present in Beijing PM$_{2.5}$ samples, and their carbon numbers ranged from C$_{27}$ to C$_{32}$ but not C$_{28}$ (Table 2). The average concentration of hopanes in Beijing was $32.7 \pm 24.7$ ng m$^{-3}$, with $15.2 \pm 10.7$ ng m$^{-3}$ and $44.6 \pm 24.6$ ng m$^{-3}$ on non-haze and haze days, respectively. Previous studies have found that C$_{29}$ (17$\alpha$(H),21$\beta$(H)-norhopane) was dominant in the hopane series and consistent with that from coal combustion (He et al., 2006), while C$_{30}$ (17$\beta$(H)21$\alpha$(H)-hopane and 17$\alpha$(H),21$\beta$(H)-hopane) was similar to C$_{29}$ in the winter time in Beijing and attributed to gasoline and diesel exhaust (Simoneit, 1985).

Levoglucosan and methoxyphenols from pyrolysis of cellulose and lignin are usually used as unique tracers for biomass burning in source apportionment models (Schauer and Cass, 2000). Levoglucosan (1,6-anhydro-$\beta$-D-glucopyranose) has been employed as the specific molecular marker for a long time for long-range transport of biomass burning aerosol, based on its high-emission factors and assumed chemical stability (Fraser and Lakshmanan, 2000; Simoneit et al., 2000). It is a highly abundant compound, and the concentrations in winter in Beijing have a significant fluctuation (Table 1). The average $\sum$levoglucosan was $355 \pm 232$ ng m$^{-3}$ during the entire sampling period, and $417 \pm 223$ ng m$^{-3}$ in haze episodes, approximately 2 times that of the non-haze days, $238 \pm 193$ ng m$^{-3}$, indicating a significant impact of biomass burning on wintertime aerosols in Beijing.

**Table 2.** Molecular formula, diagnostic ions and average concentrations of hopanes identified in PM$_{2.5}$.

| Compounds | | Molecular formula | Diagnostic ions | IAP (ng m$^{-3}$) |
|---|---|---|---|---|
| 18$\alpha$(H)22, 29, 30-Trisnorneohopane | Ts | C$_{27}$H$_{46}$ | 191/370 | 2.91 $\pm$ 3.06 |
| 17$\alpha$(H)-22,29,30-Trisnorhopane | Tm | C$_{27}$H$_{46}$ | 191/370 | 1.56 $\pm$ 2.74 |
| 17$\alpha$(H)21$\beta$(H)-30-Norhopane | 29$\alpha\beta$ | C$_{29}$H$_{50}$ | 191/398 | 9.92 $\pm$ 7.63 |
| 17$\beta$(H)21$\alpha$(H)-Hopane(Moretane) | 30$\beta\alpha$ | C$_{30}$H$_{52}$ | 191/412 | 5.77 $\pm$ 6.12 |
| 17$\alpha$(H)21$\beta$(H)-Hopane | 30$\alpha\beta$ | C$_{30}$H$_{52}$ | 191/412 | 3.71 $\pm$ 5.49 |
| 17$\alpha$(H)21$\beta$(H)-Homohopane(22R) | 30$\alpha\beta$-22R | C$_{31}$H$_{54}$ | 191/426 | 1.32 $\pm$ 1.31 |
| 17$\alpha$(H)21$\beta$(H)-Homohopane(22S) | 30$\alpha\beta$-22S | C$_{31}$H$_{54}$ | 191/426 | 0.83 $\pm$ 0.93 |
| 17$\alpha$(H), 21$\beta$(H)-Bishomohopane(22S) | 30$\alpha\beta$-22S | C$_{32}$H$_{56}$ | 191/440 | 5.23 $\pm$ 6.51 |
| 17$\alpha$(H)21$\beta$(H)-Bishomohopane(22R) | 30$\alpha\beta$-22R | C$_{32}$H$_{56}$ | 191/440 | 1.41 $\pm$ 1.73 |

Methoxyphenols are usually also considered to be tracers for wood burning (Simpson et al., 2005; Yee et al., 2013), with the average $\sum$ methoxyphenols at 7.29 $\pm$ 7.11 ng m$^{-3}$ and the haze days (9.03 $\pm$ 7.93 ng m$^{-3}$) being 2 times greater than non-haze days (4.74 $\pm$ 4.95 ng m$^{-3}$) during the campaigns. In Beijing and its surrounding areas, harvest occurs in late September to October for corn, and biomass fuels are used for cooking and heating purposes in the winter. However, the methoxyphenols are abundant components in the smoke from broadleaf tree and shrub burning (Wang et al., 2009) and have been identified in all coal smoke (Simoneit, 2002); thus they cannot be used as source-specific markers for biomass burning.

Phenolic compounds from the thermal degradation of lignin have been proposed as potentially useful tracers for wood smoke, and many of them are emitted in relatively high quantities and are specific to wood combustion sources (Simoneit, 2002; Simoneit et al., 2004). Another important source of phenolic compounds is oxidation of monoaromatic compounds and PAHs (Pan and Wang, 2014). Phenols and naphthalenol were identified in the PM$_{2.5}$, with the average $\sum$ phenolic compounds of 21.6 $\pm$ 17.0 ng m$^{-3}$, being 14.0 $\pm$ 13.2 and 25.9 $\pm$ 17.9 ng m$^{-3}$ on the non-haze and haze days, respectively. However, it is notable that the concentrations of naphthalenol identified in the present study were far lower than that of previous studies (Table 1).

Pristane (Pr) and phytane (Ph) have been found in the exhaust of petrol and diesel engines and in lubricating oil, indicating their origin from petroleum (Simoneit, 1984). Since their presence is ubiquitous in vehicle exhausts and negligible in contemporary biogenic sources in urban environments, they can be used as petroleum tracers for airborne particulate matter. The mean values of Pr and Ph in our samples are 2.24 and 1.94 ng m$^{-3}$, respectively. Biogenic inputs are often characterized by a predominance of the odd carbon alkanes and Pr. Since Ph is rarely found in biological material, most biological hydrocarbons have a Pr/Ph ratio far higher than 1.0 (Oliveira et al., 2007), but values approaching unity indicate a hydrocarbon signature derived from petrochemical use. The average Pr/Ph ratios were 1.15 for PM$_{2.5}$ samples,

and this finding is quite similar to the results from the southern Chinese city of Guangzhou, 1.1–1.8 (Bi et al., 2002), but almost 4 times greater than Beijing summer samples (0.3; Simoneit et al., 1991). The high Pr/Ph indicated that the hydrocarbons in urban aerosol derive mainly from petroleum residues, probably coming from vehicular emissions in Beijing.

### 3.4 The molecular distributions of aliphatic hydrocarbons

Figure 4 shows the molecular distributions of aliphatic hydrocarbons on non-haze and haze days. The details on the n-alkanes are given by Lyu et al. (2019a). Briefly, the $\sum$ n-alkanes (C$_{10}$–C$_{36}$) ranged from 42.4 to 1241 ng m$^{-3}$, with an average 450 $\pm$ 316 ng m$^{-3}$, and the average $\sum$ n-alkanes was 577 ng m$^{-3}$ during haze episodes, more than twice that of the non-haze period (264 ng m$^{-3}$). The n-alkanes (C$_{20}$–C$_{31}$) were the most abundant homologues (Fig. 4), accounting for approximately 83 % of the $\sum$ n-alkanes.

The total concentrations of branched alkanes (C$_{12}$–C$_{36}$) ranged from 125 to 647 ng m$^{-3}$, with the average of 356 $\pm$ 173 ng m$^{-3}$, during the sampling period. The average branched alkanes concentration was 440 $\pm$ 144 ng m$^{-3}$ during all haze episodes, which was higher than 234 $\pm$ 138 ng m$^{-3}$ on the non-haze days. The most abundant branched alkanes were observed at C$_{22}$, with the average concentration of 29.2 ng m$^{-3}$, and the greatest abundance of branched alkanes groups was observed within the carbon atom range of C$_{20}$–C$_{30}$, accounting for 67.7 % of $\sum$ branched alkanes. The branched alkanes have lower concentrations than n-alkanes when the carbon number is > C$_{20}$ on haze and non-haze days while showing higher concentrations than n-alkanes when the carbon number is lower than C$_{19}$.

It is difficult to identify the potential sources of branched alkanes from the literature, although Alam et al. (2016b) reported that branched alkanes (C$_{11}$–C$_{33}$) were an abundant compound group in diesel exhaust. The increase in HMW branched alkanes (C$_{20}$–C$_{30}$) from non-haze days to haze days is consistent with a primary emission source, probably linked to coal combustion or vehicular emissions. The

fact that both n-alkanes and branched alkanes increase quite similarly between non-haze and haze conditions is consistent with them arising from the same sources or sources with highly correlated emissions.

Other groups of aliphatic and alicyclic compounds identified in the PM$_{2.5}$ include alkyl-decalins, alkyl-pyridines, alkyl-furanones, alkyl-cyclohexanes and alkyl-benzenes. Figure 5 shows the molecular distributions of these series of compounds. Engine studies (Alam et al., 2016b) have also found that compounds observed in vehicle exhaust beside n-alkanes and PAHs include straight and branched cyclohexanes (C$_{11}$–C$_{25}$), various cyclic aromatics, alkyl-decalins, and alkyl-benzenes. The particle-bound n-C$_n$-cyclohexanes with carbon numbers from C$_{12}$ to C$_{26}$ were identified in diesel exhaust (Alam et al., 2016b), with a dominant range C$_{18}$–C$_{25}$, and the total (particle plus gas) concentration of n-C$_n$-cyclohexanes was 2.05 µg m$^{-3}$. The n-C$_n$-cyclohexanes (C$_{20}$–C$_{30}$) were identified at the IAP site with average $\sum$ n-C$_n$-cyclohexane 39.4 ± 37.1 ng m$^{-3}$. The most abundant range was observed at C$_{22}$-C$_{27}$, highly consistent with the engine study, implying a significant contribution from vehicle emissions. In addition, the average $\sum$ n-C$_n$-cyclohexane (C$_{20}$–C$_{30}$) was 53.3 ± 39.3 ng m$^{-3}$ during haze episodes, approximately 5 times higher than 10.8 ± 8.22 ng m$^{-3}$ in the non-haze period, a larger ratio than for other primary emissions. The alkyl-decalins and tetralin are products obtained by hydrogenation of naphthalene and its derivatives during the refining process and have been identified in vehicle exhaust (Afzal et al., 2008; Alam et al., 2016b; Ogawa et al., 2007). The average $\sum$ alkyl-decalins was 110 ng m$^{-3}$, with 85.4 ± 65.5 and 126 ± 110 ng m$^{-3}$ on non-haze and haze days, respectively. The $\sum$ n-C$_n$-benzene (C$_{16}$–C$_{25}$) identified in the samples ranged from 7.71 to 410 ng m$^{-3}$ with an average of 56.6 ± 73.0 ng m$^{-3}$. The average $\sum$ n-C$_n$-benzene (C$_{16}$–C$_{25}$) was 77.2 ± 88.2 ng m$^{-3}$ during haze episodes, approximately 4 times the 23.3 ± 15.1 ng m$^{-3}$ of the non-haze period. Other alkyl-benzenes (C$_9$–C$_{25}$) were also identified and have higher concentrations at C$_{12}$, especially for the non-haze days.

## 3.5 Distribution of compounds with respect to volatility and polarity, and the estimation of unidentified mass

The method for characterizing the volatility/polarity distribution of compounds is detailed in the Supplement. Briefly, the chromatography image was separated into seven parts according to the main chemical and physical properties of the organic compounds and the distribution of ISs, and the detailed protocol is shown in Table S4. The diagram of the separated image with seven parts is shown in Fig. 6a, and the concentrations measured in each part are shown in Fig. 6 and Table 3. In the chromatogram (Fig. 6), volatility decreases from left to right, and polarity increases from bottom to top. Table 3 shows the estimated mass concentration of all com-
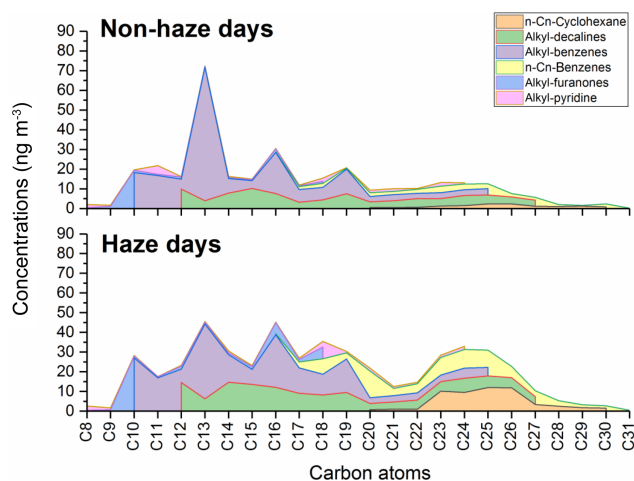


**Figure 5.** The molecular distributions of n-C$_n$-cyclohexane, alkyl-bicyclic-alkanes, alkyl-benzenes, n-C$_n$-benzenes, alkyl-furanones and alkyl-pyridines on haze and non-haze days.
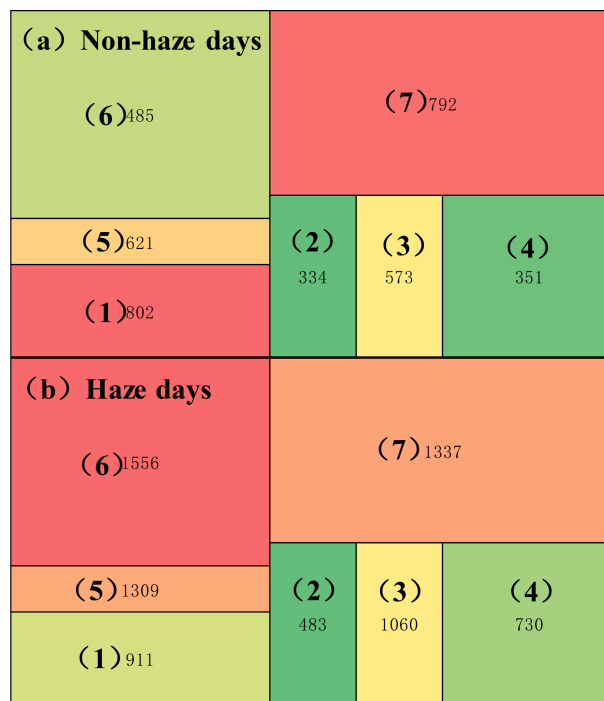


**Figure 6.** The concentration (ng m$^{-3}$) sum of identified and unknown organic compounds in each chromatogram image section during **(a)** non-haze and **(b)** haze days.

ponents of the chromatogram alongside the amount of mass not accounted for by the specific compounds reported in this paper.

For the non-haze days, the sum of identified organic compounds (IOCs) with carbon numbers higher than C$_6$ was 1.84 µg m$^{-3}$, accounting for 46.5 % of total organic compounds. The IOC of the haze days was almost 2 times that

**Table 3.** Estimated average concentrations of unknown compounds (ng m$^{-3}$) in each section of the chromatogram for haze and non-haze conditions.

| Section | Characteristics of organic compounds | Non-haze | | Haze | |
|---------|--------------------------------------|----------|--------------|-------|--------------|
| | | Total | Unidentified | Total | Unidentified |
| 1 | Low molecular weight: – Carbon numbers (n-alkanes) ≤ 17; – Monoaromatics | 802 | 546 | 911 | 632 |
| 2 | Medium molecular weight: – 17 < carbon numbers (n-alkanes) ≤ 23 – Oxidized hydrocarbons (alkanals, alkanones) | 334 | 137 | 483 | 147 |
| 3 | Medium molecular weight: – 23 < carbon numbers (n-alkanes) ≤ 27 – Oxidized hydrocarbons (alkanals and alkanones) | 573 | 215 | 1060 | 228 |
| 4 | High molecular weight: – carbon numbers (n-alkanes) ≥ 27 | 351 | 188 | 730 | 320 |
| 5 | Oxidized monoaromatics | 621 | 289 | 1309 | 985 |
| 6 | Two-ring PAHs and derivatives | 485 | 303 | 1556 | 879 |
| 7 | Three–six-ring PAHs, derivatives and hopanes | 792 | 440 | 1337 | 774 |
| | Total | 3958 | 2119 | 7385 | 3964 |

of non-haze periods, with an average of 3.42 µg m$^{-3}$, accounting for 46.3 % of total measured organic matter. In addition, the sum of unidentified compounds increased from 2.12 µg m$^{-3}$ on non-haze days to 3.96 µg m$^{-3}$ on haze days, accounting for 53.5 % and 53.7 % of total measured organic matter, respectively. Hence there is no marked difference in the proportions of identified and unidentified compounds between haze and non-haze conditions.

For the non-haze days, Section 1 of the chromatogram has the highest concentration of 802 ng m$^{-3}$, followed by Section 7 (792 ng m$^{-3}$), accounting for 20.3 % and 20.0 % of the total organic compounds, respectively, implying that both low-molecular-weight (LMW) hydrocarbons (Section 1) and HMW PAHs (Section 7; three to six rings) and compounds of similar volatility and polarity were the main organic components of atmospheric particulate matter measurable by the GC × GC separation technique. The PAHs are important organic compounds appearing in Sections 6 and 7, accounting for 32.3 % of total measured organic compounds during the non-haze days. Sections 2, 3 and 4 showed relatively low concentrations, and medium-molecular-weight hydrocarbons in the range of C$_{23}$–C$_{27}$ (Section 3) were the more abundant aliphatic hydrocarbons relative to Section 2 (C$_{17}$–C$_{23}$) and Section 4 (> C$_{27}$), probably caused by primary emissions from vehicular and coal combustion (Cao et al., 2018). Section 5 contains oxidized monoaromatic compounds, and the concentrations were higher than Section 6 (mainly containing naphthalene derivatives) and lower than Section 1, probably mainly arising from vehicular emissions or from

oxidization from the monoaromatic precursors (Section 1; Schwantes et al., 2017).

The polarity distribution characteristics of atmospheric organic compounds on the non-haze days were also studied. For the volatile areas, low-polarity compounds (Section 1) have a lower concentration than polar compounds (Sections 5 and 6) during the non-haze days. On the contrary, for the semi-and non-volatile area, the sum of low-polarity compounds (Sections 2, 3 and 4) have higher concentrations than polar organic compounds (Section 7).

The concentrations in all sections increased from non-haze to haze days, and the main difference between haze and non-haze days follows Sections 5, 6 and 7 (Fig. 6b), indicating a more polar aerosol during periods of haze. Section 6 has the highest concentrations on the haze days (1556 ng m$^{-3}$), increasing by more than threefold on the haze days in contrast to non-haze days (485 ng m$^{-3}$), followed by Section 7 (1337 ng m$^{-3}$) and Section 5 (1309 ng m$^{-3}$), indicating that the oxidized monoaromatics, naphthalene derivatives and oxidized HMW PAHs were the main identified components of the atmospheric particulate matter during the haze days. The concentrations were compared among the seven sections, and the highest concentrations of Section 6 were probably contributed by the degradation of HMW PAHs (from Section 7). For the oxidized monoaromatic compounds (Section 5), the degradation of naphthalene derivatives was probably a major contributor but not compounds oxidized from Section 1. The concentrations of Section 3 were also observed to increase from non-haze days (573 ng m$^{-3}$) to haze

days (1060 ng m$^{-3}$), indicating that accumulation has an obvious effect on the stable compounds with the carbon number between C$_{23}$ and C$_{27}$ during haze formation under low wind speed (Table S1).

## 3.6 Elevation of primary and secondary constituents during haze events

By definition, concentrations of PM$_{2.5}$ are elevated during haze events, but the question arises as to whether primary or secondary organic compounds make a larger contribution to the rise in concentrations. Constituents that are expected to be primary are typically elevated in mean concentration by a factor of around 2 (Table S3). Examples are n-alkanes (ratio of haze to non-haze of 2.2), levoglucosan (1.8) and hopanes (2.9). This is consistent with the ratios for primary gaseous emissions, including SO$_2$ (ratio of 2.6), CO (2.5) and NO$_x$ (2.2; Table S1). Surprisingly, however, both BC (ratio of 3.8) and EC (3.4; Table S1) are primary constituents with a large haze : non-haze ratio, comparable to that of PM$_{2.5}$ mass (4.0). Consequently the factors leading to an elevation of concentrations during the haze appear complex and are likely to be resolved fully only by chemistry-transport models.

OC/EC ratios are used to estimate the relative contribution of primary and secondary sources; high OC/EC ratios (> 2.0) have been observed for aerosols with significant SOA contributions in Beijing (Lv et al., 2019; Ji et al., 2018). The OC/EC ratio in this study was 3.88 on average, suggesting a significant contribution of SOA in Beijing aerosols, which is consistent with the results of Section 3.5. The aliphatic carbonyls, which have both primary and secondary sources (Lyu et al., 2019a, b), range from ratios of 1.6 (n-alkanals) to 2.8 (n-alkan-2-ones). This result was consistent with Section 3.5; it was found that the chromatogram of Sections 2 and 3, which contained alkanals (C$_{15} \le$ C$_n \le$ C$_{25}$) and alkanones (C$_{15} \le$ C$_n \le$ C$_{25}$), has slightly higher concentrations on haze days than non-haze days. However, the low-ratio alkanal and alkanone compounds are quite readily oxidized (Chacon-Madrid et al., 2010; Chacon-Madrid and Donahue, 2011), and a low ratio may reflect a high degree of further processing to form more oxidized species on the haze days, compensating for enhanced formation.

There are no compounds in Table S3 certain to be exclusively secondary. However, the results in Fig. 6 show an appreciable elevation in more polar compounds (upper part of the chromatogram) on haze days, suggestive of a greater relative abundance of more oxidized, possibly secondary compounds in the haze. The ratio of average PM$_{2.5}$ mass between haze and non-haze days was 4.0, and it was 2.7 for organic carbon (Table S1). The ratio for organic matter would be greater than 2.7 due to a higher OM/OC ratio in secondary compounds. This is strongly suggestive of a greater contribution from an elevation in secondary than primary species concentrations during the haze events and suggests that much

of the mass lies outside of the chromatogram due to the low volatility of the secondary species.

## 4 Conclusions

Over 300 polar and non-polar organic compounds were determined in the fine-particle samples from Beijing, and these compounds have been grouped into more than 20 classes, including normal and branched alkanes, n-alkenes, aliphatic carbonyl compounds (1-alkanals, n-alkan-2-ones and n-alkan-3-ones), n-alkanoic acids, n-alkanols, PAHs, oxygenated PAHs (O-PAHs), alkylated-(PAHs and O-PAHs), hopanes, n-C$_n$-benzene, alkyl-benzenes, n-C$_n$-cyclohexane, pyridines, quinolines, furanones and biomarkers (levoglucosan, cedrol, phytane, pristane, supraene and phytone). The total concentrations of identified organic compounds ranged from 0.94 to 5.14 µg m$^{-3}$, with an average of 2.84 ± 1.19 µg m$^{-3}$, accounting for 9.40 % of OM mass. The six groups which accounted for 66 % of total identified organic compound mass included n-alkanes, levoglucosan, branched alkanes, PAHs, n-alkenes and alkyl-benzenes, and these were significantly impacted by primary emission sources. In addition, the average of total polycyclic aromatic compounds (the sum of $\sum$ PAHs, $\sum$ O-PAHs, $\sum$ alkylated-(PAHs and O-PAHs), alkyl-PHE, and ANT and alkyl-NAP) was 560 ng m$^{-3}$, accounting for 1.88 % of OM. The comparisons of identified groups between non-haze and haze periods showed that most organic compound groups have a higher concentration on the haze days relative to the non-haze days. The average sum of the identified compounds increased from 1.84 to 3.42 µg m$^{-3}$ from non-haze days to haze days. A unimodal molecular distribution of alkanes was observed in the range from C$_8$ to C$_{36}$, and these compounds make significant contributions to atmospheric organic compounds in the range of C$_{19}$–C$_{28}$, especially on the haze days. The unidentified compounds in the chromatogram were estimated, and the results show that the average sum of unidentified compounds increased from 2.12 µg m$^{-3}$ on non-haze days to 3.96 µg m$^{-3}$ on haze days, accounting approximately for 53.5 % and 53.7 % of total organic compounds, respectively. Finally, the total mass concentrations of measured organic compounds ($\ge$ C$_6$) were 3.96 and 7.39 µg m$^{-3}$ on the non-haze and haze days, accounting for 26.4 % and 18.5 % of OM mass, respectively, on these days. The remaining mass is that which is not volatile under the conditions of the gas chromatography. The higher percentage of non-GC-volatile organic matter on haze days is indicative of a greater degree of oxidation of the organic aerosol, consistent with the difference in the chromatogram between haze and non-haze days. The greater contribution of secondary constituents during haze events was reported previously by Huang et al. (2014) and Ma et al. (2017) but not the greater extent of oxidation of organic matter. In a modelling study, Li et al. (2017) found that during winter haze conditions in Beijing the majority of

secondary PM$_{2.5}$ had formed 1 or more days prior to arrival, hence explaining its highly oxidized condition.

## References

Afzal, A., Chelme-Ayala, P., El-Din, A. G., and El-Din, M. G.: Automotive Wastes, Water Environ. Res., 80, 1397–1415, 2008.

Akyüz, M.: Simultaneous determination of aliphatic and aromatic amines in ambient air and airborne particulate matters by gas chromatography-mass spectrometry, Atmos. Environ., 42, 3809–3819, 2008.

Alam, M. S. and Harrison R. M.: Recent advances in the application of 2-dimensional gas chromatography with soft and hard ionisation time-of-flight mass spectrometry in environmental analysis, Chem. Sci., 7, 3968–3977, 2016.

Alam, M. S., Delgado-Saborit, J. M., Stark, C., and Harrison, R. M.: Investigating PAH relative reactivity using congener profiles, quinone measurements and back trajectories, Atmos. Chem. Phys., 14, 2467–2477, https://doi.org/10.5194/acp-14-2467-2014, 2014.

Alam, M. S., Stark, C., and Harrison, R. M.: Using variable ionisation energy time-of-flight mass spectrometry with comprehensive GC × GC to identify isomeric species, Anal. Chem., 88, 4211–4220, 2016a.

Alam, M. S., Zeraati-Rezaei, S., Stark, C. P., Liang, Z., Xu, H., and Harrison, R. M.: The characterisation of diesel exhaust particles – composition, size distribution and partitioning, Faraday. Discuss., 189, 69–84, 2016b.

Alam, M. S., Zeraati-Rezaei, S., Liang, Z., Stark, C., Xu, H., MacKenzie, A. R., and Harrison, R. M.: Mapping and quantifying isomer sets of hydrocarbons ($\geq$C$_{12}$) in diesel exhaust, lubricating oil and diesel fuel samples using GC × GC-ToF-MS, Atmos. Meas. Tech., 11, 3047–3058, https://doi.org/10.5194/amt-11-3047-2018, 2018.

Bi, X., Sheng, G., Peng, P. A., Zhang, Z., and Fu, J.: Extractable organic matter in PM$_{10}$ from LiWan District of Guangzhou City, PR China, Sci. Total Environ., 300, 213–228, 2002.

Botalova, O., Schwarzbauer, J., Frauenrath, T., and Dsikowitzky, L.: Identification and chemical characterization of specific organic constituents of petrochemical effluents, Water Res., 43, 3797–3812, 2009.

Cao, R., Zhang, H., Geng, N., Fu, Q., Teng, M., Zou, L., Gao, Y., and Chen, J.: Diurnal variations of atmospheric polycyclic aromatic hydrocarbons (PAHs) during three sequent winter haze episodes in Beijing, China, Sci. Total Environ., 625, 1486–1493, 2018.

Cass, G. R.: Organic molecular tracers for particulate air pollution sources, TrAC Trends Anal. Chem., 17, 356–366, 1998.

Chacon-Madrid, H. J. and Donahue, N. M.: Fragmentation vs. functionalization: chemical aging and organic aerosol formation, Atmos. Chem. Phys., 11, 10553–10563, https://doi.org/10.5194/acp-11-10553-2011, 2011.

Chacon-Madrid, H. J., Presto, A. A., and Donahue, N. M.: Functionalization vs. fragmentation: n-aldehyde oxidation mechanisms and secondary organic aerosol formation, Phys. Chem. Chem. Phys., 12, 13975–13982, 2010.

Chiavari, G. and Galletti, G. C.: Pyrolysis – gas chromatography/mass spectrometry of amino acids, J. Anal. Appl. Pyrol., 24, 123–137, 1992.

Ding, J., Zhong, J., Yang, Y., Li, B., Shen, G., Su, Y., Chen, W., Shen, H., Wang, B., and Rong, W.: Occurrence and exposure to polycyclic aromatic hydrocarbons and their derivatives in a rural chinese home through biomass fuelled cooking, Environ. Pollut., 169, 160–166, 2012.

Fan, X., Wei, S., Zhu, M., Song, J., and Peng, P. A.: Molecular characterization of primary humic-like substances in fine smoke particles by thermochemolysis–gas chromatography–mass spectrometry, Atmos. Environ., 180, 1–10, 2018.

Fraser, M. P. and Lakshmanan, K.: Using levoglucosan as a molecular marker for the long-range transport of biomass combustion aerosols, Environ. Sci. Technol., 34, 4560–4564, 2000.

Gao, Y., Guo, X., Ji, H., Li, C., Ding, H., Briki, M., Tang, L., and Zhang, Y.: Potential threat of heavy metals and PAHs in PM$_{2.5}$ in different urban functional areas of Beijing, Atmos. Res., 178, 6–16, 2016.

Guo, S., Hu, M., Guo, Q., Zhang, X., Schauer, J. J., and Zhang, R.: Quantitative evaluation of emission controls on primary and secondary organic aerosol sources during Beijing 2008 Olympics, Atmos. Chem. Phys., 13, 8303–8314, https://doi.org/10.5194/acp-13-8303-2013, 2013.

Hamilton, J. F., Webb, P. J., Lewis, A. C., Hopkins, J. R., Smith, S., and Davy, P.: Partially oxidised organic components in urban aerosol using GCXGC-TOF/MS, Atmos. Chem. Phys., 4, 1279–1290, https://doi.org/10.5194/acp-4-1279-2004, 2004.

Haque, Md. M., Kawamura, K., Deshmukh, D. K., Fang, C., Song, W., Mengying, B., and Zhang, Y.-L.: Characterization of organic aerosols from a Chinese megacity during winter: predominance of fossil fuel combustion, Atmos. Chem. Phys., 19, 5147–5164, https://doi.org/10.5194/acp-19-5147-2019, 2019.

Harrison, R. M., Alam, M. S., Dang, J., Ismail, I., Basahi, J., Alghamdi, M. A., Hassan, I., and Khoder, M.: Relationship of polycyclic aromatic hydrocarbons with oxy (quinone) and nitro derivatives during air mass transport, Sci. Tot. Environ., 572, 1175–1183, 2016.

He, L.-Y., Hu, M., Huang, X.-F., Zhang, Y.-H., and Tang, X.-Y.: Seasonal pollution characteristics of organic compounds in atmospheric fine particles in Beijing, Sci. Total Environ., 359, 167–176, 2006.

Hendricker, A. D. and Voorhees, K. J.: Amino acid and oligopeptide analysis using Curie-point pyrolysis mass spectrometry with in-situ thermal hydrolysis and methylation: mechanistic considerations, J. Anal. Appl. Pyrol., 48, 17–33, 1998.

Huang, R.-J., Zhang Y., Bozzetti, C., Ho, F.-H., Cao, J.-J., Han, Y., Daellenbach, K. R., Slowik, J. G., Platt, S. M., Canonaco, F., Zotter, P., Wolf, R., Pieber, S. M., Bruns, E. A., Crippa, M., Ciarelli, G., Piazzalunga, A., Schwikowski, M., Abbaszade, G., Schnelle-Kreis, J., Zimmermann, R., An, Z., Szidat, S., Baltensperger, U., El Haddad, I., and Prevot, A. S. H.: High secondary aerosol contribution to particulate pollution during haze events in China, Nature, 514, 218–222, 2014.

Huang, X.-F., He, L.-Y., Hu, M., and Zhang, Y.-H.: Annual variation of particulate organic compounds in PM$_{2.5}$ in the urban atmosphere of Beijing, Atmos. Environ., 40, 2449–2458, 2006.

Keyte, I. J., Harrison, R. M., and Lammel, G.: Chemical reactivity and long-range transport potential of polycyclic aromatic hydrocarbons – a review, Chem. Soc. Rev., 42, 9333–9391, 2013.

Ji, D., Yan, Y., Wang, Z., He, J., Liu, B., Sun, Y., Gao, M., Li, Y., Cao, W., Cui, Y., Hu, B., Xin, J., Wang, L., Liu, Z., Tang, G., and Wang, Y.: Two-year continuous measurements of carbonaceous aerosols in urban Beijing, China: Temporal variations, characteristics and source analyses, Chemosphere, 200, 191–200, 2018.

Kögel-Knabner, I.: $^{13}$C and $^{15}$N NMR spectroscopy as a tool in soil organic matter studies, Geoderma, 80, 243–270, 1997.

Kong, S., Ji, Y., Liu, L., Chen, L., Zhao, X., Wang, J., Bai, Z., and Sun, Z.: Spatial and temporal variation of phthalic acid esters (PAEs) in atmospheric PM$_{10}$ and PM$_{2.5}$ and the influence of ambient temperature in Tianjin, China, Atmos. Environ., 74, 199–208, 2013.

Lang, J., Zhang, Y., Zhou, Y., Cheng, S., Chen, D., Guo, X., Chen, S., Li, X., Xing, X., and Wang, H.: Trends of PM$_{2.5}$ and chemical composition in Beijing, 2000–2015, Aerosol Air Qual. Res., 17, 412–425, 2017.

Li, L. J., Ho, S. S. H., Feng, B., Xu, H., Wang, T., Wu, R., Huang, W., Qu, L., Wang, Q., and Cao, J.: Characterization of particulate-bound polycyclic aromatic compounds (PACs) and their oxidations in heavy polluted atmosphere: A case study in urban Beijing, China during haze events, Sci. Total Environ., 660, 1392–1402, 2019.

Li, J. and Wang, G.: Airborne particulate endocrine disrupting compounds in China: Compositions, size distributions and seasonal variations of phthalate esters and bisphenol A, Atmos. Res., 154, 138–145, https://doi.org/10.1016/j.atmosres.2014.11.013, 2015.

Li, J., Du, H., Wang, Z., Sun, Y., Yang, W., Li, J., Tang, X., and Fu, P.: Rapid formation of a severe regional winter haze episode over a mega-city cluster on the North China Plain, Environ. Pollut., 223, 605–615, 2017.

Lin, Y., Ma, Y., Qiu, X., Li, R., Fang, Y., Wang, J., Zhu, Y., and Hu, D.: Sources, transformation, and health implications of PAHs and their nitrated, hydroxylated, and oxygenated derivatives in PM$_{2.5}$ in Beijing, J. Geophys. Res.-Atmos., 120, 7219–7228, https://doi.org/10.1002/2015JD023628, 2015.

Lv, D., Chen, Y., Zhu, T., Li, T., Shen, F., and Li X.: The pollution characteristics of PM$_{10}$ and PM$_{2.5}$ during summer and winter in Beijing, Suning and Islamabad, Atmos. Pollut. Res., 10, 1159–1164, https://doi.org/10.1016/j.apr.2019.01.021, 2019.

Lyu, R. and Harrison, R.: Organic compounds in particulate matter from Beijing, University of Birmingham, https://doi.org/10.25500/edata.bham.00000303, 2019.

Lyu, R., Shi, Z., Alam, M. S., Wu, X., Liu, D., Vu, T. V., Stark, C., Fu, P., Feng, Y., and Harrison, R. M.: Alkanes and aliphatic carbonyl compounds in wintertime PM$_{2.5}$ in Beijing, China, Atmos. Environ., 202, 244–255, https://doi.org/10.1016/j.atmosenv.2019.01.0232019, 2019a.

Lyu, R., Alam, M. S., Stark, C., Xu, R., Shi, Z., Feng, Y., and Harrison, R. M.: Aliphatic carbonyl compounds (C$_8$–C$_{26}$) in wintertime atmospheric aerosol in London, UK, Atmos. Chem. Phys., 19, 2233–2246, https://doi.org/10.5194/acp-19-2233-2019, 2019b.

Ma, Y., Cheng, Y., Qiu, X., Cao, G., Fang, Y., Wang, J., Zhu, T., Yu, J., and Hu, D.: Sources and oxidative potential of water-soluble humic-like substances (HULISWS) in fine particulate matter (PM$_{2.5}$) in Beijing, Atmos. Chem. Phys., 18, 5607–5617, https://doi.org/10.5194/acp-18-5607-2018, 2018.

Ma, Q., Wu, Y., Zhang, D., Wang, X., Xia, Y., Liu, X., Tian, P., Han, Z., Xia, X., Wang, Y., and Zhang, R.: Roles of regional transport and heterogeneous reactions in the PM$_{2.5}$ increase during winter haze episodes in Beijing, Sci. Total Environ., 599–600, 246–253, 2017.

Ogawa, H., Ibuki, T., Minematsu, T., and Miyamoto, N.: Diesel combustion and emissions of decalin as a high productivity gas-to-liquid fuel, Energ. Fuel., 21, 1517–1521, 2007.

Oliveira, T. S., Pio, C., Alves, C. A., Silvestre, A. J., Evtyugina, M., Afonso, J., Fialho, P., Legrand, M., Puxbaum, H., and Gelencsér, A.: Seasonal variation of particulate lipophilic organic compounds at nonurban sites in Europe, J. Geophys. Res.-Atmos., 112, D23S09, https://doi.org/10.1029/2007JD008504, 2007.

Oros, D. and Simoneit, B.: Identification and emission rates of molecular tracers in coal smoke particulate matter, Fuel, 79, 515–536, 2000.

Pan, S. and Wang, L.: Atmospheric oxidation mechanism of m-xylene initiated by OH radical, J. Phys. Chem. A, 118, 10778–10787, 2014.

Pitts, J. N., Lokensgard, D. M., Ripley, P. S., Van Cauwenberghe, K. A., Van Vaeck, L., Shaffer, S. D., Thill, A. J., and Belser, W. L.: Atmospheric epoxidation of benzo[a]pyrene by ozone: Formation of the metabolite benzo[a]pyrene-4, 5-oxide, Science, 210, 1347–1349, 1980.

Ren, L., Fu, P., He, Y., Hou, J., Chen, J., Pavuluri, C. M., Sun, Y., and Wang, Z.: Molecular distributions and compound-specific stable carbon isotopic compositions of lipids in wintertime aerosols from Beijing, Sci. Rep.-UK, 6, 27481, https://doi.org/10.1038/srep27481, 2016.

Ringuet, J., Albinet, A., Leoz-Garziandia, E., Budzinski, H., and Villenave, E.: Reactivity of polycyclic aromatic compounds (PAHs, NPAHs and OPAHs) adsorbed on natural aerosol particles exposed to atmospheric oxidants, Atmos. Environ., 61, 15–22, 2012.

Rogge, W. F., Hildemann, L. M., Mazurek, M. A., Cass, G. R., and Simoneit, B. R. T.: Sources of fine organic aerosol. 2. Noncatalyst and catalyst-equipped automobiles and heavy-duty diesel trucks, Environ. Sci. Technol., 27, 636–651, 1993a.

Rogge, W. F., Mazurek, M. A., Hildemann, L. M., Cass, G. R., and Simoneit, B. R. T.: Quantification of urban organic aerosols at a molecular level: Identification, abundance and seasonal variation, Atmos. Environ. A-Gen., 27, 1309–1330, 1993b.

Rogge, W. F., Hildemann, L. M., Mazurek, M. A., Cass, G. R., and Simoneit, B. R. T.: Sources of Fine Organic Aerosol. 6. Cigaret Smoke in the Urban Atmosphere, Environ. Sci. Technol., 28, 1375–1388, 1994.

Schauer, J. J. and Cass, G. R.: Source apportionment of wintertime gas-phase and particle-phase air pollutants using organic compounds as tracers, Environ. Sci. Technol., 34, 1821–1832, 2000.

Schauer, J. J., Rogge, W. F., Hildemann, L. M., Mazurek, M. A., Cass, G. R., and Simoneit, B. R. T.: Source apportionment of airborne particulate matter using organic compounds as tracers, Atmos. Environ., 30, 3837–3855, 1996.

Schmitter, J., Ignatiadis, I., and Arpino, P.: Distribution of diaromatic nitrogen bases in crude oils, Geochim. Cosmochim. Ac., 47, 1975–1984, 1983.

Schwantes, R. H., Schilling, K. A., McVay, R. C., Lignell, H., Coggon, M. M., Zhang, X., Wennberg, P. O., and Seinfeld, J. H.: Formation of highly oxygenated low-volatility products from cresol oxidation, Atmos. Chem. Phys., 17, 3453–3474, https://doi.org/10.5194/acp-17-3453-2017, 2017.

Shakya, K. M. and Griffin, R. J.: Secondary organic aerosol from photooxidation of polycyclic aromatic hydrocarbons, Environ. Sci. Technol., 44, 8134–8139, 2010.

Shen, G., Tao, S., Wang, W., Yang, Y., Ding, J., Xue, M., Min, Y., Zhu, C., Shen, H., and Li, W.: Emission of oxygenated polycyclic aromatic hydrocarbons from indoor solid fuel combustion, Environ. Sci. Technol., 45, 3459–3465, 2011.

Shen, G., Tao, S., Wei, S., Zhang, Y., Wang, R., Wang, B., Wei, L. I., Shen, H., Huang, Y., and Chen, Y.: Emissions of parent, nitro, and oxygenated polycyclic aromatic hydrocarbons from residential wood combustion in rural China, Environ. Sci. Technol., 46, 8123–8130, 2012a.

Shen, G., Wei, S., Zhang, Y., Wang, R., Wang, B., Li, W., Shen, H., Huang, Y., Chen, Y., and Chen, H.: Emission of oxygenated polycyclic aromatic hydrocarbons from biomass pellet burning in a modern burner for cooking in China, Atmos. Environ., 60, 234–237, 2012b.

Shen, R., Schäfer, K., Schnelle-Kreis, J., Shao, L., Norra, S., Kramar, U., Michalke, B., Abbaszade, G., Streibel, T., Zimmermann, R., and Emeis, S.: Seasonal variability and source distribution of haze particles from a continuous one-year study in Beijing, Atmos. Pollut. Res., 9, 627–633, 2018.

Shi, Z., Vu, T., Kotthaus, S., Harrison, R. M., Grimmond, S., Yue, S., Zhu, T., Lee, J., Han, Y., Demuzere, M., Dunmore, R. E., Ren, L., Liu, D., Wang, Y., Wild, O., Allan, J., Acton, W. J., Barlow, J., Barratt, B., Beddows, D., Bloss, W. J., Calzolai, G., Carruthers, D., Carslaw, D. C., Chan, Q., Chatzidiakou, L., Chen, Y., Crilley, L., Coe, H., Dai, T., Doherty, R., Duan, F., Fu, P., Ge, B., Ge, M., Guan, D., Hamilton, J. F., He, K., Heal, M., Heard, D., Hewitt, C. N., Hollaway, M., Hu, M., Ji, D., Jiang, X., Jones, R., Kalberer, M., Kelly, F. J., Kramer, L., Langford, B., Lin, C., Lewis, A. C., Li, J., Li, W., Liu, H., Liu, J., Loh, M., Lu, K., Lucarelli, F., Mann, G., McFiggans, G., Miller, M. R., Mills, G., Monk, P., Nemitz, E., O'Connor, F., Ouyang, B., Palmer, P. I., Percival, C., Popoola, O., Reeves, C., Rickard, A. R., Shao, L., Shi, G., Spracklen, D., Stevenson, D., Sun, Y., Sun, Z., Tao, S., Tong, S., Wang, Q., Wang, W., Wang, X., Wang, X., Wang, Z., Wei, L., Whalley, L., Wu, X., Wu, Z., Xie, P., Yang, F., Zhang, Q., Zhang, Y., Zhang, Y., and Zheng, M.: Introduction to the special issue "In-depth study of air pollution sources and processes within Beijing and its surrounding region (APHH-Beijing)", Atmos. Chem. Phys., 19, 7519–7546, https://doi.org/10.5194/acp-19-7519-2019, 2019.

Simoneit, B. R. T.: Organic matter of the troposphere – III. Characterization and sources of petroleum and pyrogenic residues in aerosols over the western united states, Atmos. Environ., 18, 51–67, 1984.

Simoneit, B. R.: Application of molecular marker analysis to vehicular exhaust for source reconciliations, Int. J. Environ. An. Ch., 22, 203–232, 1985.

Simoneit, B. R. T.: Biomass burning – a review of organic tracers for smoke from incomplete combustion, Appl. Geochem., 17, 129–162, 2002.

Simoneit, B. R. and Mazurek, M. A.: Organic matter of the troposphere – II. Natural background of biogenic lipid matter in aerosols over the rural western united states, Atmos. Environ., 16, 2139–2159, 1982.

Simoneit, B., Schnoes, H., Haug, P., and Burlingame, A.: High-resolution mass spectrometry of nitrogenous compounds of the Colorado Green River Formation oil shale, Chem. Geol., 7, 123–141, 1971.

Simoneit, B. R. T., Sheng, G., Chen, X., Fu, J., Zhang, J., and Xu, Y.: Molecular marker study of extractable organic matter in aerosols from urban areas of China, Atmos. Environ., 25, 2111–2129, 1991.

Simoneit, B., Rogge, W., Lang, Q., and Jaffé, R.: Molecular characterization of smoke from campfire burning of pine wood (Pinus elliottii), Chemosphere-Global Change Sci., 2, 107–122, 2000.

Simoneit, B. R. T., Kobayashi, M., Mochida, M., Kawamura, K., Lee, M., Lim, H.-J., Turpin, B. J., and Komazaki, Y.: Composition and major sources of organic compounds of aerosol particulate matter sampled during the

ACE-Asia campaign, J. Geophys. Res.-Atmos., 109, D19S10, https://doi.org/10.1029/2004JD004598, 2004.

Simpson, C. D., Paulsen, M., Dills, R. L., Liu, L. J. S., and Kalman, D. A.: Determination of methoxyphenols in ambient atmospheric particulate matter:? Tracers for wood combustion, Environ. Sci. Technol., 39, 631–637, 2005.

Staples, C. A., Peterson, D. R., Parkerton, T. F., and Adams, W. J.: The environmental fate of phthalate esters: a literature review, Chemosphere, 35, 667–749, 1997.

Sun, Y. L., Wang, Z. F., Fu, P. Q., Yang, T., Jiang, Q., Dong, H. B., Li, J., and Jia, J. J.: Aerosol composition, sources and processes during wintertime in Beijing, China, Atmos. Chem. Phys., 13, 4577–4592, https://doi.org/10.5194/acp-13-4577-2013, 2013.

Turpin, B. J. and Lim, H.-J.: Species contributions to PM$_{2.5}$ mass concentrations: Revisiting common assumptions for estimating organic mass, Aerosol Sci. Tech., 35, 602–610, 2001.

Wang, G. and Kawamura, K.: Molecular characteristics of urban organic aerosols from Nanjing: A case study of a mega-city in China, Environ. Sci. Technol., 39, 7430–7438, 2005.

Wang, G., Kawamura, K., Lee, S., Ho, K., and Cao, J.: Molecular, seasonal, and spatial distributions of organic aerosols from fourteen Chinese cities, Environ. Sci. Technol., 40, 4619–4625, 2006.

Wang, J., Ho, S. S. H., Huang, R., Gao, M., Liu, S., Zhao, S., Cao, J., Wang, G., Shen, Z., and Han, Y.: Characterization of parent and oxygenated-polycyclic aromatic hydrocarbons (PAHs) in Xi'an, China during heating period: An investigation of spatial distribution and transformation, Chemosphere, 159, 367–377, https://doi.org/10.1016/j.chemosphere.2016.06.033, 2016.

Wang, W.: Regional distribution and air-soil exchange of polycyclic aromatic hydrocarbons (PAHs) and their derivatives in Beijing-Tianjin area, PhD Dissertation, Peking University, Beijing, China, 2010.

Wang, Z., Bi, X., Sheng, G., and Fu, J.: Characterization of organic compounds and molecular tracers from biomass burning smoke in South China I: Broad-leaf trees and shrubs, Atmos. Environ., 43, 3096–3102, 2009.

Wei, S., Huang, B., Liu, M., Bi, X., Ren, Z., Sheng, G., and Fu, J.: Characterization of PM$_{2.5}$-bound nitrated and oxygenated PAHs in two industrial sites of South China, Atmos. Res., 109, 76–83, 2012.

Welthagen, W., Schnelle-Kreis, J., and Zimmermann, R.: Search criteria and rules for comprehensive two-dimensional gas chromatography–time-of-flight mass spectrometry analysis of airborne particulate matter, J. Chromatogr. A, 1019, 233–249, 2003.

Wu, X., Vu, T. V., Shi, Z., Harrison, R. M., Liu, D., and Cen, K.: Characterization and Source Apportionment of Carbonaceous PM$_{2.5}$ Particles in China – A Review, Atmos. Environ., 189, 187–212, 2018.

Yao, L., Yang, L., Yuan, Q., Yan, C., Dong, C., Meng, C., Sui, X., Yang, F., Lu, Y., and Wang, W.: Sources apportionment of PM$_{2.5}$ in a background site in the North China Plain, Sci. Total Environ., 541, 590–598, 2016.

Yee, L. D., Kautzman, K. E., Loza, C. L., Schilling, K. A., Coggon, M. M., Chhabra, P. S., Chan, M. N., Chan, A. W. H., Hersey, S. P., Crounse, J. D., Wennberg, P. O., Flagan, R. C., and Seinfeld, J. H.: Secondary organic aerosol formation from biomass burning intermediates: phenol and methoxyphenols, Atmos. Chem. Phys., 13, 8019–8043, https://doi.org/10.5194/acp-13-8019-2013, 2013.

Zhang, Q., Anastasio, C., and Jimenez-Cruz, M.: Water-soluble organic nitrogen in atmospheric fine particles (PM$_{2.5}$) from northern California, J. Geophys. Res.-Atmos., 107, 4112, https://doi.org/10.1029/2001JD000870, 2002.

Zhang, Y.-X., Shao, M., Zhang, Y.-H., Zeng, L.-M., He, L.-Y., Zhu, B., Wei, Y., and Zhu, X.: Source profiles of particulate organic matters emitted from cereal straw burnings, J. Environ. Sci., 19, 167–175, 2007.

Zhao, J., Peng, P. A., Song, J., Ma, S., Sheng, G., and Fu, J.: Characterization of organic matter in total suspended particles by thermodesorption and pyrolysis-gas chromatography-mass spectrometry, J. Environ. Sci., 21, 1658–1666, 2009.

Zhou, J., Wang, T., Zhang, Y., Zhong, N., Medeiros, P. M., Simoneit, B. R. T.: Composition and sources of organic matter in atmospheric PM$_{10}$ over a two year period in Beijing, China, Atmos. Res., 93, 849–861, 2009.